RESEARCH ARTICLE
SPACE PHYSICS

Earth and Planetary Physics
7: 540–547, 2023
doi: 10.26464/epp2023050

Comparative analysis of extreme ultraviolet solar radiation proxies during minimum activity levels

A. G. Elias[1,2*], C. R. Martinis[3], B. F. de Haro Barbas[1], F. D. Medina[1,2], B. S. Zossi[1,2], M. Fagre[4,5], and T. Duran[6,7]

[1]Laboratorio de Ionosfera, Atmosfera Neutra y Magnetosfera, Facultad de Ciencias Exactas y Tecnologia (FACET), Universidad Nacional de Tucuman (UNT), Tucuman 4000, Argentina;

[2]Instituto de Física del Noroeste Argentino, Consejo Nacional de Investigaciones Cientificas y Tecnicas (CONICET)-UNT, Tucuman 4000, Argentina;

[3]Center for Space Physics, Astronomy Department, Boston University, MA 02215, USA;

[4]CONICET, Tucuman 4000, Argentina;

[5]Laboratorio de Telecomunicaciones, Departamento de Electricidad, Electrónica y Computación, FACET, UNT, Tucuman, 4000, Argentina;

[6]Departamento de Física, Universidad Nacional del Sur (UNS), Bahia Blanca 8000, Argentina;

[7]Instituto de Física del Sur, CONICET-UNS, Bahia Blanca 8000, Argentina

Key Points:

- Solar extreme ultraviolet (EUV) proxies that are highly correlated throughout a solar cycle, or for longer periods, become less similar during minimum activity level epochs.
- The minima between cycles 23 and 24, and cycles 24 and 25 are both weaker than previous minimum periods, according to the EUV proxies.
- The MgII and Lyman α flux represent EUV radiation levels better than do the *Rz* and $F_{10.7}$ indices during the last two unusual minima.

Citation: Elias, A. G., Martinis, C. R., de Haro Barbas, B. F., Medina, F. D., Zossi, B. S., Fagre, M., and Duran, T. (2023). Comparative analysis of extreme ultraviolet solar radiation proxies during minimum activity levels. *Earth Planet. Phys.*, *7*(5), 540–547. http://doi.org/10.26464/epp2023050

Abstract: Four extreme ultraviolet (EUV) solar radiation proxies (Magnesium II core-to-wing ratio (MgII), Lyman α flux (F_α), 10.7-cm solar radio flux ($F_{10.7}$), and sunspot number (*Rz*)) were analyzed during the last four consecutive solar activity minima to investigate how they differ during minimum periods and how well they represent solar EUV radiation. Their variability within each minimum and between minima was compared by considering monthly means. A comparison was also made of their role in filtering the effect of solar activity from the critical frequency of the ionospheric F_2 layer, f_oF_2, which at mid to low latitudes depends mainly on EUV solar radiation. The last two solar cycles showed unusually low EUV radiation levels according to the four proxies. Regarding the connection between the EUV "true" variation and that of solar proxies, according to the f_oF_2 filtering analysis, MgII and F_α behaved in a more stable and suitable way, whereas *Rz* and $F_{10.7}$ could be overestimating EUV levels during the last two minima, implying they would both underestimate the inter-minima difference of EUV when compared with the first two minima.

Keywords: solar EUV radiation; solar minimum; f_oF_2; solar activity; solar EUV proxy

1. Introduction

The solar extreme ultraviolet (EUV) electromagnetic radiation covering wavelengths between 10 and 120 nm is absorbed in the terrestrial thermosphere, leading to photoionization and the formation of the ionosphere, as well as heating and increased neutral density (Rishbeth and Garriott, 1969). Because it is absorbed in the upper atmosphere, EUV radiation is not observable from the ground, so when satellite measurements are not available, its variation is determined from proxies. The sunspot number (*Rz*), 10.7-cm solar radio flux ($F_{10.7}$), Magnesium II core-to-wing ratio (MgII), and Lyman *α* solar flux (F_α) are some of the solar EUV proxies used by the solar–terrestrial community.

Emissions at EUV wavelengths typically originate in the top layers of the solar atmosphere. This can be observed in Figure 1, where the height associated with several solar ultraviolet (UV) emissions is identified (Vernazza et al., 1981; Lean, 1987). For wavelengths shorter than 120 nm, the solar spectrum is dominated by a chromospheric transition region and coronal emissions. However, each of the four aforementioned indices originates in a more specific region of the Sun. From the lowest region to the highest, sunspots occur in the solar photosphere, MgII in the chromosphere, F_α in a wide range of heights in the solar chromosphere, and $F_{10.7}$ in the solar corona.

Over long time scales, solar activity has usually been studied by *Rz*,

Correspondence to: A. G. Elias, aelias@herrera.unt.edu.ar
Received 30 DEC 2022; Accepted 13 JUN 2023.
First Published online 14 JUL 2023.

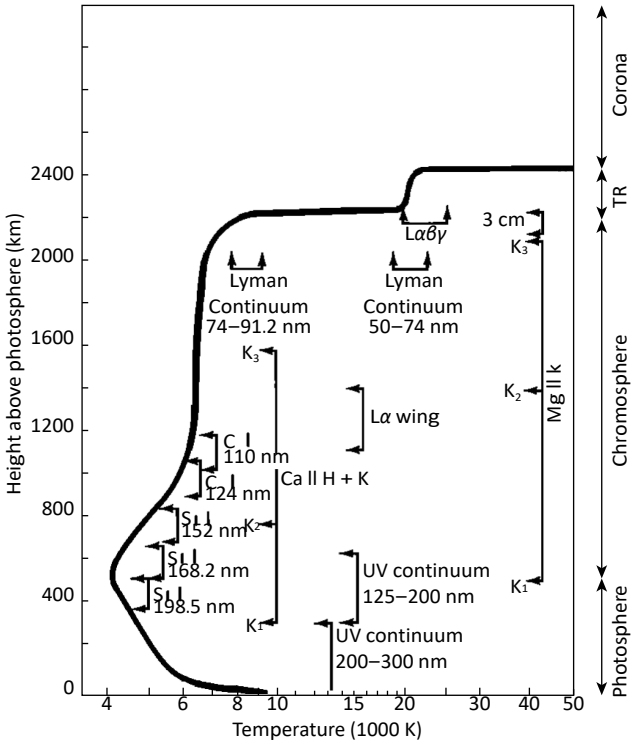

Figure 1. The temperature distribution of the average quiet Sun, indicating approximate depths of formation of various solar emissions (from Lean, 1987). TR, transition region.

which has been available since the 1600s (Vaquero, 2007). Its main periodicity is the quasi-decadal cycle, and most solar parameters, not only *Rz*, also follow this cycle. Accordingly, in years of high solar activity, when more sunspots are seen, the Sun emits more radiation in most spectral ranges, including the EUV, whereas in periods of minima with the least sunspots, the Sun emits less radiation (Lukianova and Mursula, 2011).

The main variation in EUV solar proxies with the resolution of a month (i.e., monthly mean time series) or greater is related to the quasi-decadal solar cycle. The linear correlation between any pair of solar proxies is greater than 0.95 at this time scale when a period covering a complete activity cycle or longer is considered (Elias et al., 2021). However, when shorter periods are considered, particularly during minimum activity levels, this correlation decreases (Bruevich et al., 2014; Okoh and Okoro, 2020; Elias et al., 2021).

Another aspect that has become noteworthy since the last two solar activity minima is the difference between their values when comparing different epochs of minimum activity levels. The minimum between solar activity cycles 23 and 24 was remarkable by its long duration and the very low values observed for different solar activity indices in comparison with previous cycles (Solomon et al., 2010, 2013; Clette and Lefevre, 2012; Luhmann et al., 2013; Russell et al., 2013). In addition, the "true" solar EUV levels would be different from those deduced from its proxies, such as *Rz* and $F_{10.7}$ (Emmert et al., 2010; Chen YD et al., 2011). The last minimum, between cycles 24 and 25, was also quite low.

In this work, *Rz*, $F_{10.7}$, MgII, and F_α were studied comparatively during the last four consecutive solar activity minima to analyze the differences among these solar EUV proxies around minimum periods and determine how well they represent solar EUV radiation. This study is based on monthly mean time series, where we expect them to behave more similarly. At shorter time scales, the correlation between them becomes poor because the day-to-day evolution of each parameter is more likely governed by different physical processes that take place at different heights in the solar atmosphere (Wintoft, 2011). Because solar EUV emissions are the source of the bulk of the ionosphere, a comparison was also made of their role in filtering the effect of solar activity from the critical frequency of the ionospheric F_2 layer, f_oF_2, a parameter representing the peak electron density that at mid to low latitudes depends mainly on EUV solar radiation. Hence, we analyzed the variation in f_oF_2 residuals, which was defined as the f_oF_2 values after filtering the effects of solar activity. This process may serve as a tool to detect possible failures of the proxies as indicators of the real variability in the solar EUV during minimum epochs, providing another analytical perspective on these particular periods.

Previous studies have used ionospheric parameters as a measure of solar EUV to analyze inter-minimum variations, but they have not included the latest minimum occurring between solar cycles 24 and 25, or they have considered different aspects of the ionospheric response. Lee (2016) and Mikhailov and Perrone (2018), for example, considered the F_1-layer critical frequency, f_oF_1. In a later work, Ippolito et al. (2020) analyzed storm-linked f_oF_2 anomalies. Chen YD et al. (2011), Huang JP et al. (2017), and Liu LB et al. (2021) also analyzed the F_2 layer as an EUV-sensitive system to closely examine minimum solar activity levels. However, the latest minimum considered by all these works was that between cycles 23 and 24. Nusinov et al. (2021) developed EUV and far-UV models of the quiet Sun for aeronomic purposes, which covered the complete solar cycle 24 but without focusing on an inter-minimum comparison. Deminov et al. (2021) analyzed solar cycles 23 and 24 by considering $F_{10.7}$ and *Rz*, which focused on the shape features of the complete cycles, especially of the maximum.

The novel contribution of our work is twofold. First, we include the most recent minimum between cycles 24 and 25, which to our knowledge has not yet been discussed comparatively with previous minima. Second, we provide an additional aspect to the comparative analysis by including the f_oF_2 trend analysis.

2. Data

Four solar activity proxies and ionosonde data from six midlatitude stations, three in Japan and three in Australia, were considered in this study. The solar activity proxies are as follows:

(1) MgII: the ratio of the H and K lines of the solar MgII emission at 280 nm to the background solar continuum near 280 nm. This ratio serves as a proxy for UV and EUV spectral solar irradiance variability. We used the composite MgII, also called the Bremen composite MgII index, which combines data from different satellites and is available from the University of Bremen (Viereck et al., 2010; Snow et al., 2014).

(2) F_α (in W/m^2 units): the full disk integrated solar irradiance over 121–122 nm, dominated by the solar Hydrogen I 121.6 nm emis-

sion. We used the composite F_α, which combines multiple instruments and models, available from the Laboratory for Atmospheric and Space Physics (LASP, University of Colorado) Interactive Solar Irradiance Data Center (LISIRD) (Machol et al., 2019).

(3) $F_{10.7}$ (in solar flux units (sfu) = 10^{-22} Ws/m^2): the radio emission from the Sun at a wavelength of 10.7 cm (2800 MHz), measured at the Earth's surface at the Penticton Radio Observatory in British Columbia, Canada.

(4) *Rz*: a revised sunspot number, obtained from the Sunspot Index and Long-term Solar Observations (SILSO), Royal Observatory of Belgium, Brussels.

Monthly means of MgII and F_α were estimated from their daily databases, whereas $F_{10.7}$ and *Rz* monthly values were obtained directly from their data sources. Taking into account that the MgII dataset is the shortest data series, beginning at the end of 1978, we considered the period from January 1979 to December 2020 for all proxies for ionospheric filtering analysis. In addition, from these time series, the last four minimum solar activity periods were separated, corresponding to minima between cycles 21 and 22 (min21–22), 22 and 23 (min22–23), 23 and 24 (min23–24), and 24 and 25 (min24–25) for the direct comparative analysis.

In the case of ionospheric data, monthly median f_oF_2 values from three Japanese stations — Kokubunji (35.7°N, 139.5°E), Wakkanai (45.4°N, 141.7°E), and Okinawa (26.31°N, 127.59°E) — and three Australian stations — Canberra (35.17°S, 149.08°E), Townsville (19.16°S, 146.48°E), and Hobart (42.53°S, 147.19°E) — were chosen because their data record had the least number of gaps during the period analyzed here. Data were provided by the World Data Centre (WDC) for Ionosphere and Space Weather, Tokyo, National Institute of Information and Communications Technology (NICT), in the case of the Japanese stations, and by the WDC for Space Weather, Australia, for the Australian stations. The critical frequency f_oF_2 was obtained from a manually scaled database that had 1-hour sampling. For consistency, the same period from January 1979 to December 2020 of the solar activity proxies was considered. Noontime f_oF_2 values were obtained by averaging median values between 11 and 14 local time. During this time of day, solar EUV radiation is at a maximum; thus, the best linear association with ionospheric parameters was expected.

3. Methodology and Results

3.1 Direct Comparative Analysis Between Periods of Minimum Solar Activity

For this comparative analysis, monthly means and 12-month running means were considered. The latter case corresponds to the low-pass filtered series where intra-annual variability was filtered out.

Before the inter-minimum comparison, we present some characteristics that distinguish each EUV proxy time series. We analyzed each proxy sensitivity along the solar activity cycle through its variation in terms of percentage. For this analysis, the amplitude of the decadal cycle relative to the mean value considering the corresponding cycle was estimated as

$$100\ [X\ \mathrm{max}\ X\ \mathrm{min}] \blacktriangledown \mathrm{mean}\ X,$$

where *X* represents each EUV proxy, and *X*(max) and *X*(min) correspond to the maximum and minimum value, respectively, for each of the four cycles covered by the period considered. In other words, "sensitivity" is interpreted here as the response of the proxy to the variation between the maximum and the minimum level of solar activity. To be able to conduct a comparison between proxies, we expressed the sensitivity as a percentage with respect to the average value during the complete cycle. From highest to lowest, the average percentage sensitivity was ~250% for *Rz*, ~120% for $F_{10.7}$, ~45% for F_α, and 10% for MgII. Two extreme cases were noted: *Rz*, for which the amplitude of variation in a cycle was two and a half times that of its average value, and MgII, for which this amplitude was of the order of one tenth of its average value.

Through a linear correlation analysis, the temporal behavior of each proxy could be compared. Figure 2 shows, as an example, the dispersion diagram between *Rz* and MgII by considering monthly means. An almost ideal linear association was observed, as revealed by the high correlation coefficient, which was greater than 0.95.

This high correlation occurred in the cases when all pairs between the four EUV indices were considered (six in total). However, this almost perfect correlation was not stable along the solar activity cycle when subperiods were considered. Elias et al. (2021) analyzed the correlation between pairs of proxies for subperiods, based on work by Bruevich et al. (2014), by going through the different phases of the solar cycle and "isolating" minimum periods, which are the focus of this work. They observed that the correlation coefficient in all the cases presented a marked decrease around maximum and minimum periods. This means that around periods of minima and maxima, the temporal behavior of different solar EUV proxies was not as similar within each period.

We then made a comparison among the different minima. Figure 3 shows the superposition for each proxy when the 12-

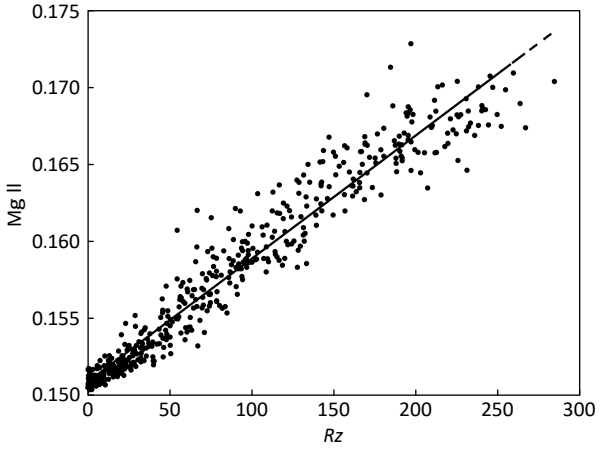

Figure 2. Dispersion diagram between monthly mean values of MgII and *Rz* when considering the period from January 1979 to December 2020. The black line is the least squares linear fit.

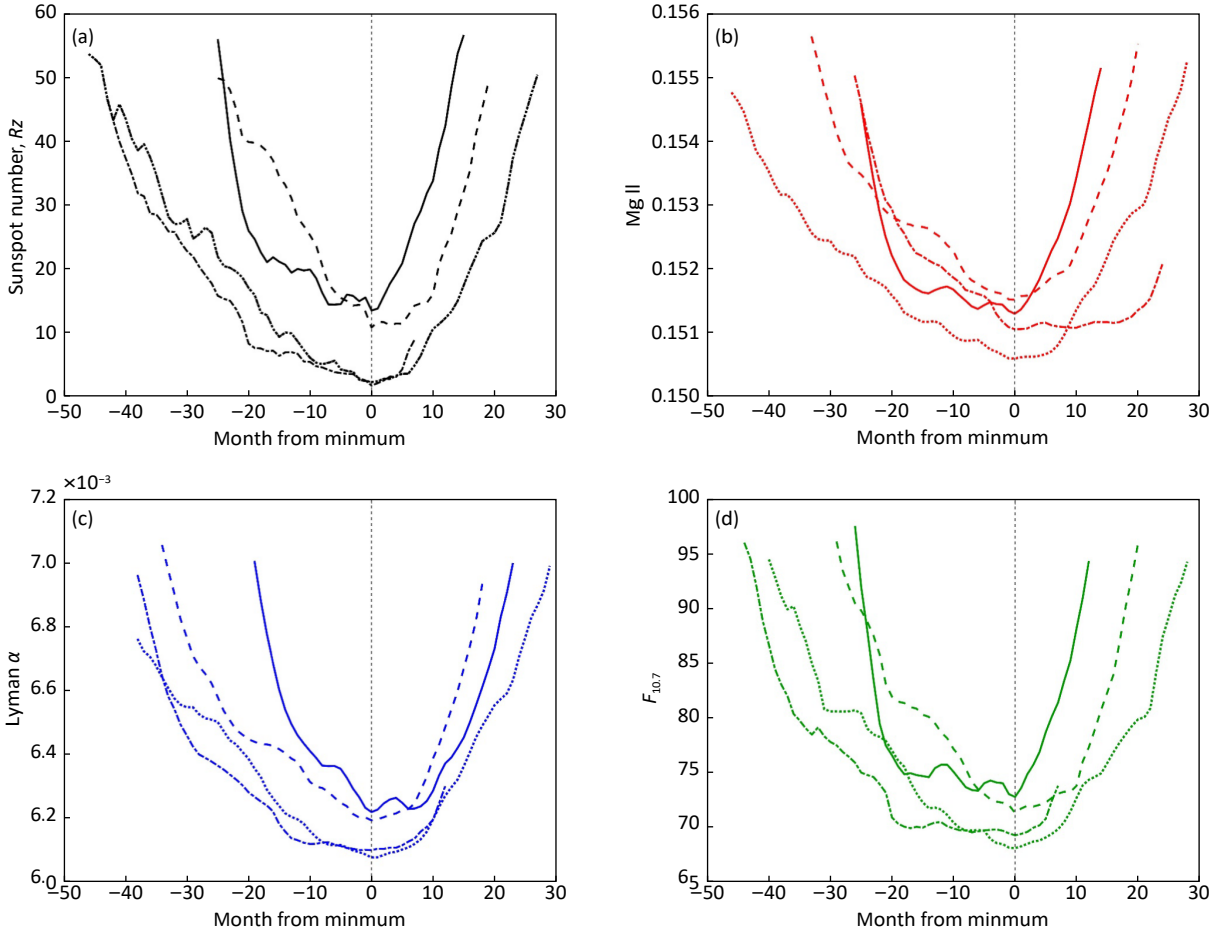

Figure 3. Superposition of (a) *Rz* (black), (b) MgII (red), (c) F_α (blue), and (d) $F_{10.7}$ (green) in a 12-month running mean series during solar cycle minimum periods: min21–22 (solid line), min22–23 (dashed line), min23–24 (dotted line), and min24–25 (dotted-dashed line). Zero corresponds to the minimum value in each case.

month running mean series was considered, where zero corresponds to the date of the minimum value within each period. To delimit the curves, the *Rz* value of 55 was chosen so that the minimum period was completely covered during the four minima considered. The equivalent of this *Rz* value was used for the cases of the other proxies. In this way, each curve in Figure 3 satisfied the condition $Rz < 55$, MgII < 0.156, $F_\alpha < 0.0071$, and $F_{10.7} < 97$. It is clear from this figure, as is well known, that the descending phase is longer than the ascending phase. Two main features are the weakest last two minima in comparison with the previous two, which also last longer, and the difference in the exact date of the minimum within a given minimum, depending on the proxy considered.

Table 1 presents the minimum value attained by each proxy in the different minima, together with the corresponding date. Here we confirm not only that min23–24 and min24–25 were the lowest, but also that there was a difference between dates. The period min23–24 was the only one with a common date for the minimum value of all proxies. Regarding the last two minima, min23–24 was lower than min24–25, except for the case of *Rz*. We could argue here that *Rz* had a lower limit (which was zero) too close to its minimum value and thus it could not go lower, even when the EUV radiation levels were much lower than in any previous minimum period. Note also that the difference between the lowest *Rz* value in min23–24 and min24–25 is small.

3.2 Comparative Analysis Between Periods of Minimum Solar Activity Through the Ionosphere

The time variability in the 12-month running means of monthly medians of f_oF_2 can be analyzed by considering that f_oF_2 is a direct effect of solar EUV variation. In fact, the linear correlation for periods longer than a complete solar cycle is again greater than 0.95, revealing a close linear association. Actually, f_oF_2 is a measure of the maximum ionospheric electron density, which occurs around a height of 300 km and depends directly on solar EUV radiation, which is the main ionization source, especially at mid and low latitudes. It should be noted that in analyzing the 12-month running mean, all shorter timescale variations, which can be stronger than those linked to solar activity, were filtered out, as would be the case for seasonality and transient variation from different sources (gravity waves from below, geomagnetic activity, and others).

A key aspect of long-term trend assessments in ionospheric parameters is the solar activity filtering from the 12-month running mean or annual time series prior to the trend estimation (Laštovička, 2019, 2021a; Huang JP et al., 2020; de Haro Barbás, 2021). We analyzed f_oF_2 filtering with each EUV proxy for the

Table 1. Date of the minimum value (columns 2–5) and the minimum value (columns 6–9) of each minimum period for each solar extreme ultraviolet proxy.

Solar minimum	Cycle minimum date				Cycle minimum value			
	Rz	MgII	F_{α}	$F_{10.7}$	*Rz*	MgII	F_{α}	$F_{10.7}$
min21–22	1986.6	1986.7	1986.2	1986.7	13.38	0.1513	0.00622	72.8
min22–23	1996.3	1996.3	1996.5	1996.3	10.72	0.1515	0.00619	71.3
min23–24	2008.8	2008.8	2008.8	2008.8	2.19	0.1506	0.00608	68.1
min24–25	2019.8	2018.4	2019.4	2019.9	1.65	0.1510	0.00610	69.3

different subperiods to detect the efficiency of each proxy in eliminating the solar EUV radiation effect from f_oF_2, and from here we deduced the true variation in this solar spectral radiation. By "true variation," we mean the real solar EUV spectral variation. We should keep in mind that *Rz*, $F_{10.7}$, MgII, and F_{α} are merely proxies. Thus, they tell us how EUV varies through their own variation.

The f_oF_2 filtering was done in the usual way, which was by estimating the residuals from a linear regression between f_oF_2 and each EUV proxy (Laštovička, 2021b) as follows:

$$f_oF_2 \text{ residual} \quad f_oF_{2exp} \quad AX \; B, \tag{1}$$

where f_oF_{2exp} is the measured f_oF_2 data, *X* stand for the solar proxy (*Rz*, $F_{10.7}$, MgII, or F_{α}), and *A* and *B* are the least squares parameters of the linear regression between f_oF_{2exp} and *X*.

Aside from the expected trends in these residuals, namely, decreasing trends attributable to increasing concentrations of greenhouse gases, long-term variation in geomagnetic activity, and secular variation in the Earth's magnetic field, the lack of agreement between the variation in proxies and that of true solar EUV radiation should induce an additional trend according to the following:

• If EUV is higher than the level indicated by solar proxies during the last two minima, then trends estimated including these periods should be more positive than those without them.

• If EUV is lower than the level indicated by solar proxies during the last two minima, then trends estimated including these periods should be more negative than those without them.

• If EUV behaves like the solar proxies during the last two minima, then we should see the same trend despite whether the last two minima are included.

Figure 4 shows the trend values estimated from the linear regression between f_oF_2 residuals and time for each of the six ionospheric stations. The residuals and their trends were assessed by considering each EUV proxy for four different periods, namely, the entire period from 1979 to 2020 (case 1, blue bars), and this same period but excluding the first two minimum subperiods (min21–22 and min22–23; case 2, orange bars), excluding all the minimum subperiods (case 3, gray bars), and excluding the last two minimum subperiods (min23–24 and min24–25; case 4, yellow bars). Each excluded minimum period was ~2 to ~3 years long, with its center being the minimum date. This was done with the expectation that if only during the last two minima the EUV was not well represented by the proxies, cases 1 and 2 should present similar trend values.

Cases 3 and 4 should also be similar, but with more positive or more negative trends than cases 1 and 2, depending on the proxies underestimating or overestimating the solar EUV, respectively, during these last two minima. In the six ionospheric stations analyzed here (Kokubunji, Wakkanai, Okinawa, Canberra, Townsville, and Hobart), it was clear that if *Rz* was used as a proxy to filter solar EUV, the trend results would be more positive. And although it is not recommended in f_oF_2 filtering for trend analysis (Laštovička, 2021a), it still explains ~95% of the variance in f_oF_2. Thus, it is useful for our comparative analysis, in which we are focusing on the adequacy of its role within a filtering procedure. Residuals obtained with MgII and with F_{α} yielded more stable trend values (more similar among the four cases), except for Townsville, where all the proxies yielded rather different trends among cases 1 to 4. In focusing on the comparison between periods for each proxy, we observed that in most cases, it was clear that cases 3 and 4 (gray and yellow bars) were less negative than cases 1 and 2 (blue and orange bars). This also occurred systematically in the cases of *Rz* and $F_{10.7}$, with the only exception being at Wakkanai. Hence, according to our previous reasoning, this would mean that *Rz* and $F_{10.7}$ overestimated EUV levels during the last two minima. The other two proxies seemed to behave similarly, but our results are not conclusive in these cases.

4. Discussion and Conclusions

Correlation coefficients between any pair of solar EUV proxies selected in this study, for the period from 1979 to 2020, were greater than 0.95. When we focused on shorter periods, the coefficients decreased, specifically during the maximum and minimum periods, as previously shown by Bruevich et al. (2014) and Elias et al. (2021). The good agreement in variability among all EUV proxies (with a monthly resolution) then decreased within a minimum activity level period. One reason for this could be purely statistical, as explained by Elias et al. (2021), or, considering that the variation linked to the quasi-decadal cycle is minimal at these levels of activity (the first derivatives are zero because we are at a maximum or minimum of the curves), the time variation attributable to specific forcings of each proxy gains relative importance, and these do not need to be correlated among the different indices. These unrelated time variations within a minimum (or maximum) period are weak compared with the complete quasi-decadal variation, so they lose importance during the rising and falling phases of a solar activity cycle. But within the ~3-year period or less, which can last through a period of minimum activity and during which the quasi-decadal cycle is at its trough, short-term inter-monthly variations suppresses the correlation.

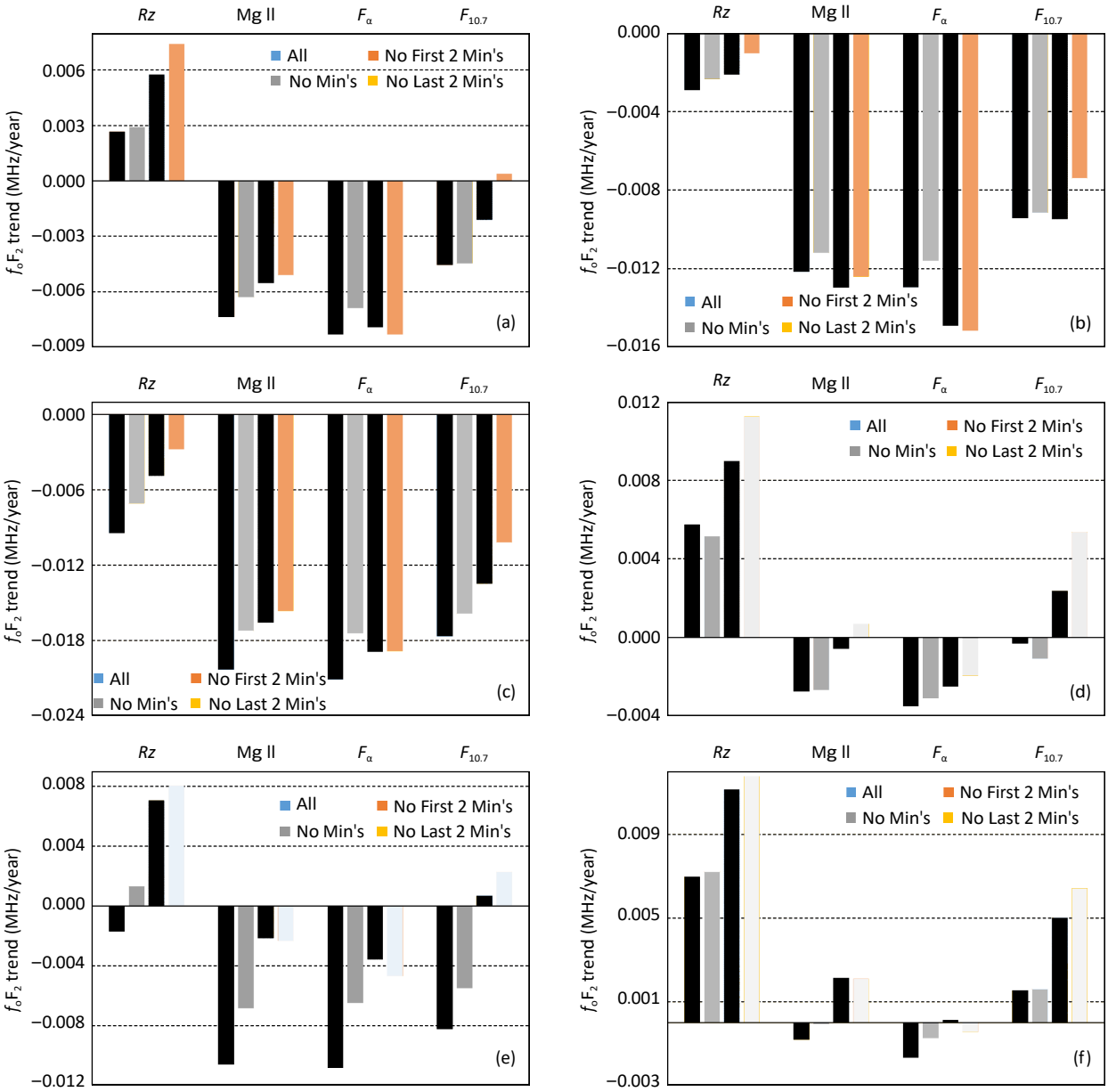

Figure 4. Linear trend for the critical frequency of the ionospheric F_2 layer (f_oF_2) residuals for (a) Kokubunji (35.7°N, 139.5°E), (b) Wakkanai (45.4°N, 141.7°E), (c) Okinawa (26.31°N, 127.59°E), (d) Canberra (35.17°S, 149.08°E), (e) Townsville (19.16°S, 146.48°E), and (f) Hobart (42.53°S, 147.19°E) obtained after filtering *Rz*, MgII, F_α, and $F_{10.7}$ when considering the whole period from 1979 to 2020 (All, blue bars), the whole period excluding the first two minimum periods (No First 2 Min's, orange bars), the whole period excluding all minimum periods (No Min's, gray bars), and the whole period excluding the last two minimum periods (No Last 2 Min's, yellow bars).

Following the comparison of EUV levels between minimum periods, the superposed epoch analysis (Figure 3) clearly showed that the last two minima had lower EUV radiation levels than did the first two, together with a longer duration. This was already observed by several authors, especially in the case of min23–24 (Luhmann et al., 2012). In addition, each minimum was lower than the previous one, except MgII for the first two periods. When we assessed the percentage decrease of each relative to the first, that is, of min22–23, min23–24, and 24–25 relative to min21–22, even though the differences between minima were all similar, the difference was the greatest for *Rz* followed by $F_{10.7}$, as can be deduced from Table 1. This result should be linked to the greater sensitivity of these proxies, something already noted by Bruevich and Bruevich (2019) in the case of $F_{10.7}$ and highlighted as a convenient characteristic of certain calculations and interpretations.

With respect to the minimum duration, as shown in Figure 3, the descending phases of min23–24 and min24–25 were similar except for MgII, where min23–24 was clearly the longest. In fact, the length of cycle 23 was ~2 years longer than usual, whereas cycle 24 did not show a significant lengthening with respect to previous cycles (Miyahara et al., 2021).

Regarding the trend results, MgII and F_α (which varied less with

the solar activity cycle) seemed to produce the most stable f_oF_2 trends. Trends obtained when *Rz* was considered in the filtering process were more unstable. We can conclude, based on these results, that MgII and F_α would play a better role as a solar true measure of EUV and that *Rz* would be the worst, followed by $F_{10.7}$. This result is in agreement with the greatest percentage difference in *Rz* and $F_{10.7}$ inter-minima, which seemed not to be detected by f_oF_2, possibly implying that the real difference in EUV solar radiation is greater than that indicated by these two solar proxies.

We can now contextualize the novel contributions of this work, as mentioned at the end of Section 1. Regarding the first contribution, namely, the inclusion of the most recent minimum in the comparative analysis, Bruevich et al. (2019) and Bruevich and Yakunina (2019) were among the few works to have included the complete solar cycle 24. The first study investigated the variation in EUV along the different cycle phases in comparison with solar cycle 23, and the latter one closely examined cycle 24. Bruevich et al. (2018) also analyzed solar EUV along solar cycle 24, highlighting its weaker maximum in comparison with cycles 22 and 23. Bruevich and Bruevich (2019) considered several solar activity proxies within a 40-year-long analysis that included the full 24th cycle. They detected different trends among them since 1990 and a sharp decrease in the last 40 years, which they linked to a possible association with a decrease in the intensity of large-scale magnetic fields in the solar photosphere and in the corona. In any case, none of these studies discussed the comparison of the most recent minimum with the previous one that occurred in 2008, as in this work.

Regarding our second contribution of the comparative analysis through studying the f_oF_2 trend, some studies have performed an inter-minimum analysis by using ionospheric parameters but overall have not addressed the points we are addressing here. Lee (2016) and Mikhailov and Perrone (2018) considered the F_1-layer critical frequency, f_oF_1; however, the latest minimum period they considered was between cycles 23 and 24. Lee (2016) analyzed min22–23 and min23–24 but found no differences in f_oF_1 between these two minima, even though the solar activity was lower in the latter. In contrast, Mikhailov and Perrone (2018) observed inter-minimum f_oF_1 changes whose magnitude depended on the station and the period analyzed. The minimal f_oF_1 was observed in 2008–2009. In addition, through the analysis of storm-linked f_oF_2 anomalies, Ippolito et al. (2020) confirmed the results presented by Mikhailov and Perrone (2018), showing that the deep solar minimum of 2008–2009 was actually the lowest among the last six solar cycle minima in terms of EUV fluxes. Hence, none of these works included min24–25 in their comparative analysis, as was also the case for Chen YD et al. (2011), Huang JP et al. (2017), and Liu LB et al. (2021). By considering the time series up to December 2020 in this work, it was possible to carry out a comparative analysis of the most recent minimum, between cycles 24 and 25.

In summary, on a monthly frequency, *Rz*, $F_{10.7}$, MgII, and F_α varied similarly when a complete solar cycle, or a longer period, was considered. For periods covering only minimum activity levels, this similarity between proxies decreased. Regarding their accuracy in representing the variability in solar EUV radiation, MgII and F_α seemed to be more precise since the minimum between solar cycles 23 and 24, that is, since 2008, with *Rz* and $F_{10.7}$ possibly overestimating EUV radiation levels during the last two minimum periods. This result implies that *Rz* and $F_{10.7}$ would underestimate the inter-minimum difference in EUV when compared with the first two minima. As novel contributions, the most recent minimum between cycles 24 and 25 was analyzed comparatively with previous minimum periods, and the solar EUV levels during all these minima were analyzed through an ionospheric trend analysis not previously considered.

Acknowledgments

A.G. Elias, B.S. Zossi, and F.D. Medina acknowledge Research Project Numbers PIUNT E642 and PIP 2957. The work of C. Martinis was supported by National Science Foundation Grant Number AGS-2152365.

Open Research

Ionospheric data from the Wakkanai, Kokubunji, and Okinawa stations are available from the WDC for Ionosphere and Space Weather, Tokyo, NICT, at https://wdc.nict.go.jp/IONO/index_E.html and http://wdc.nict.go.jp/IONO/HP2009/ISDJ/manual_txt-E.html, and ionospheric data from the Canberra, Townsville, and Hobart stations are available from the WDC for Space Weather, Australia, at https://downloads.sws.bom.gov.au/wdc/iondata/au/. The composite MgII index is available from the University of Bremen at http://www.iup.uni-bremen.de/UVSAT/datasets/mgii. The composite Lyman α is available from the LASP Interactive Solar Irradiance Data Center, University of Colorado, at https://lasp.colorado.edu/data/timed_see/composite_lya/ lyman_alpha_composite.nc. Data for $F_{10.7}$ are available from Space Weather Canada at https://spaceweather.gc.ca/forecast-prevision/solar-solaire/solarflux/sx-en.php. Data for *Rz* are available from SILSO, Royal Observatory of Belgium, Brussels, at http://www.sidc.be/silso/datafiles.

References

Bruevich, E., and Bruevich, V. (2019). Long-term trends in solar activity. Variations of solar indices in the last 40 years. *Res. Astron. Astrophys.*, *19*(7), 090. https://doi.org/10.1088/1674-4527/19/7/90

Bruevich, E. A., Bruevich, V. V., and Yakunina, G. V. (2014). Changed relation between solar 10.7-cm radio flux and some activity indices which describe the radiation at different altitudes of atmosphere during cycles 21–23. *J. Astrophys. Astron.*, *35*(1), 1–15. https://doi.org/10.1007/s12036-014-9258-0

Bruevich, E. A., Bruevich, V. V., and Yakunina, G. V. (2018). Cyclic variations in the solar radiation fluxes at the beginning of the 21st century. *Moscow Univ. Phys. Bull.*, *73*(2), 216–222. https://doi.org/10.3103/S0027134918020030

Bruevich, E. A., Kazachevskaya, T. V., and Yakunina, G. V. (2019). Variations of solar EUV radiation fluxes in hydrogen lines from observations by the TIMED satellite in cycle 23 and by *SDO/EVE* in cycle 24. *Geomagn. Aeron.*, *59*(8), 1048–1054. https://doi.org/10.1134/S0016793219080024

Bruevich, E. A., and Yakunina, G. V. (2019). Flux variations in lines of solar EUV radiation beyond flares in cycle 24. *Geomagn. Aeron.*, *59*(2), 155–161. https://doi.org/10.1134/S0016793219020038

Chen, Y. D., Liu, L. B., and Wan, W. X. (2011). Does the $F_{10.7}$ index correctly describe solar EUV flux during the deep solar minimum of 2007–2009?. *J. Geophys. Res.*: *Space Phys.*, *116*(A4), A04304. https://doi.org/10.1029/2010JA016301

Clette, F., and Lefevre, L. (2012). Are the sunspots really vanishing? Anomalies in solar cycle 23 and implications for long-term models and proxies. *J. Space Weather Space Clim.*, *2*, A06. https://doi.org/10.1051/swsc/2012007

de Haro Barbás, B. F., Elias, A. G., Venchiarutti, J. V., Fagre, M., Zossi, B. S., Jun, G. T., and Medina, F. D. (2021). MgII as a solar proxy to filter F2-region ionospheric parameters. *Pure Appl. Geophys.*, *178*(11), 4605–4618. https://doi.org/10.1007/s00024-021-02884-y

Deminov, M. G., Deminov, R. G. and Nepomnyashchaya, E. V. (2021). Solar-activity indices for the ionosphere in cycles 23 and 24: The form of cycles. *Geomagn. Aeron.*, *61*(Suppl 1), S75–S79. https://doi.org/10.1134/S0016793222010054

Elias, A. G., de Haro Barbas, B. F., Medina, F. D., and Zossi, B. S. (2021). On the correlation between EUV solar radiation proxies and their long-term association. In *Proceedings of the Thirteenth Workshop "Solar Influences on the Magnetosphere, Ionosphere and Atmosphere"* (pp. 20–23). Sofia, Bulgaria.

Emmert, J. T., Lean, J. L., and Picone, J. M. (2010). Record-low thermospheric density during the 2008 solar minimum. *Geophys. Res. Lett.*, *37*(12), L12102. https://doi.org/10.1029/2010GL043671

Huang, J. P., Hao, Y. Q., Zhang, D. H., and Xiao, Z. (2017). Revisiting interminima solar EUV change using adjusted SOHO SEM data. *J. Geophys. Res.*: *Space Phys.*, *122*(3), 3420–3429. https://doi.org/10.1002/2016JA023664

Huang, J. P., Hao, Y. Q., Zhang, D. H., and Xiao, Z. (2020). The use of monthly mean average for investigating the presence of hysteresis and long-term trends in ionospheric *NmF*2. *J. Geophys. Res.*: *Space Phys.*, *125*(1), e2019JA026905. https://doi.org/10.1029/2019JA026905

Ippolito, A., Perrone, L., Plainaki, C., and Cesaroni, C. (2020). Investigating the f_oF_2 variations at the ionospheric observatory of Rome during different solar cycles minimums and levels of geomagnetic activity. *J. Space Weather Space Clim.*, *10*, 52. https://doi.org/10.1051/swsc/2020054

Laštovička, J. (2019). Is the relation between ionospheric parameters and solar proxies stable?. *Geophys. Res. Lett.*, *46*(24), 14208–14213. https://doi.org/10.1029/2019GL085033

Laštovička, J. (2021a). The best solar activity proxy for long-term ionospheric investigations. *Adv. Space Res.*, *68*(6), 2354–2360. https://doi.org/10.1016/j.asr.2021.06.032

Laštovička, J. (2021b). Long-term trends in the upper atmosphere. In W. B. Wang, et al. (Eds.), *Upper Atmosphere Dynamics and Energetics* (pp. 325–341). Washington, DC: American Geophysical Union. https://doi.org/10.1002/9781119815631.ch17

Lean, J. (1987). Solar ultraviolet irradiance variations: A review. *J. Geophys. Res.*: *Atmos.*, *92*(D1), 839–868. https://doi.org/10.1029/JD092iD01p00839

Lee, C. C. (2016). Comparison of F_1 layer critical frequency between recent two solar minimums. *J. Geophys. Res.*: *Space Phys.*, *121*(9), 9090–9098. https://doi.org/10.1002/2016JA023026

Liu, L. B., Chen, Y. D., and Le, H. J. (2021). Response of the ionosphere to varying solar fluxes. In W. B. Wang, et al. (Eds.), *Upper Atmosphere Dynamics and Energetics* (pp. 301–324). Washington, DC: American Geophysical Union. https://doi.org/10.1002/9781119815631.ch16

Luhmann, J., Lee, C. O., Riley, P., Jian, L. K., Russell, C. T., and Petrie, G. (2012). Interplanetary conditions: Lessons from this minimum. In *Proceedings of the International Astronomical Union, Volume 7, Symposium S286: Comparative Magnetic Minima: Characterizing Quiet Times in the Sun and Stars* (pp. 168–178). Cambridge: Cambridge University Press. https://doi.org/10.1017/S1743921312004802

Luhmann, J. G., Petrie, G., and Riley, P. (2013). Solar origins of solar wind properties during the cycle 23 solar minimum and rising phase of cycle 24. *J. Adv. Res.*, *4*(3), 221–228. https://doi.org/10.1016/j.jare.2012.08.008

Lukianova, R., and Mursula, K. (2011). Changed relation between sunspot numbers, solar UV/EUV radiation and TSI during the declining phase of solar cycle 23. *J. Atmos. Solar-Terr. Phys.*, *73*(2–3), 235–240. https://doi.org/10.1016/j.jastp.2010.04.002

Machol, J., Snow, M., Woodraska, D., Woods, T., Viereck, R., and Coddington, O. (2019). An improved Lyman-alpha composite. *Earth Space Sci.*, *6*(12), 2263–2272. https://doi.org/10.1029/2019EA000648

Mikhailov, A. V., and Perrone, L. (2018). Interminimum f_oF_1 differences and their physical interpretation. *J. Geophys. Res.*: *Space Phys.*, *123*(1), 768–780. https://doi.org/10.1002/2017JA024831

Miyahara, H., Tokanai, F., Moriya, T., Takeyama, M., Sakurai, H., Horiuchi, K., and Hotta, H. (2021). Gradual onset of the Maunder Minimum revealed by high-precision carbon-14 analyses. *Sci. Rep.*, *11*, 5482. https://doi.org/10.1038/s41598-021-84830-5

Nusinov, A. A., Kazachevskaya, T. V., and Katyushina, V. V. (2021). Solar extreme and far ultraviolet radiation modeling for aeronomic calculations. *Remote Sens.*, *13*(8), 1454. https://doi.org/10.3390/rs13081454

Okoh, D., and Okoro, E. (2020). On the relationships between sunspot number and solar radio flux at 10.7 centimeters. *Sol. Phys.*, *295*(1), 1. https://doi.org/10.1007/s11207-019-1566-8

Rishbeth, H., and Garriott, O. K. (1969). *Introduction to Ionospheric Physics*. New York: Academic Press.

Russell, C. T., Jian, L. K., and Luhmann, J. G. (2013). How unprecedented a solar minimum was it?. *J. Adv. Res.*, *4*(3), 253–258. https://doi.org/10.1016/j.jare.2012.08.011

Snow, M., Weber, M., Machol, J., Viereck, R., and Richard, E. (2014). Comparison of Magnesium II core-to-wing ratio observations during solar minimum 23/24. *J. Space Weather Space Clim.*, *4*, A04. https://doi.org/10.1051/swsc/2014001

Solomon, S. C., Woods, T. N., Didkovsky, L. V., Emmert, J. T., and Qian, L. Y. (2010). Anomalously low solar extreme-ultraviolet irradiance and thermospheric density during solar minimum. *Geophys. Res. Lett.*, *37*(16), L16103. https://doi.org/10.1029/2010GL044468

Solomon, S. C., Qian, L. Y., and Burns, A. G. (2013). The anomalous ionosphere between solar cycles 23 and 24. *J. Geophys. Res.*: *Space Phys.*, *118*(10), 6524–6535. https://doi.org/10.1002/jgra.50561

Vaquero, J. M. (2007). Historical sunspot observations: A review. *Adv. Space Res.*, *40*(7), 929–941. https://doi.org/10.1016/j.asr.2007.01.087

Vernazza, J. E., Avrett, E. H., and Loeser, R. (1981). Structure of the solar chromosphere. III. Models of the EUV brightness components of the quiet sun. *Astrophys. J. Suppl. Ser.*, *45*, 635–725. https://doi.org/10.1086/190731

Viereck, R. A., Snow, M., DeLand, M. T., Weber, M., Puga, L., and Bouwer, D. (2010). Trends in solar UV and EUV irradiance: An update to the MgII Index and a comparison of proxies and data to evaluate trends of the last 11-year solar cycle . In *AGU Fall Meeting Abstracts*. San Francisco, CA: AGU.

Wintoft, P. (2011). The variability of solar EUV: A multiscale comparison between sunspot number, 10.7 cm flux, LASP MgII index, and SOHO/SEM EUV flux. *J. Atmos. Solar-Terr. Phys.*, *73*(13), 1708–1714. https://doi.org/10.1016/j.jastp.2011.03.009